# Prediction equations for nonlinear SDOF response from the ITalian ACcelerometric Archive: preliminary results.

Flavia De Luca, Iunio Iervolino
*Dipartimento di Ingegneria Strutturale DIST – Università degli Studi di Napoli Federico II. Via Claudio 21, 80125 Napoli.*

Gabriele Ameri, Francesca Pacor
*Istituto Nazionale di Geofisica e Vulcanologia INGV. Via Bassini 15, 20133 Milano.*

Dino Bindi
*Deutsches GeoForschungsZentrum GFZ, Centre for Disaster Managment (CEDIM), Telegrafenberg, 14473 Potsdam, Germany.*

*Keywords: ITACA, attenuation models, peak inelastic response, cyclic inelastic response, PBEE.*

ABSTRACT

Modern earthquake resistant design procedures are based on inelastic deformation of structures as the primary source of seismic energy dissipation. On the other hand, design actions are based on probabilistic seismic hazard analysis (PSHA), which refers to elastic acceleration response spectrum ordinates. Reconciliation between reference elastic demand and required inelastic performance is made via relationships calibrated on single degree of freedom (SDoF) systems, developed in the last decades and widely adopted by codes (mostly in approximate forms). Recently, is earning interest the possibility to develop PSHA directly in terms of nonlinear structural response to improve accuracy in definition of structural design targets. This may require a prediction equation (also referred to as *attenuation model*) for the structural response measure of interest. In this paper, the possibility to develop an attenuation law for nonlinear SDOF responses based on the recent Italian Accelerometric Archive (ITACA) is explored. Other than being specifically based on Italian data, the study has the advantage of considering more than one hysteretic loops, at different oscillation periods, for one strength reduction factor. Moreover, cyclic response is also considered, together with prediction of peak structural deformation. Interestingly, preliminary results indicate that standard deviation of residuals is practically not changing passing from elastic to inelastic response.

## 1 INTRODUCTION

It is easy to recognize that seismic design would benefit of hazard expressed in terms of nonlinear structural performance. In fact, currently, the conversion of common ground motion intensity measures (IMs), such as elastic spectral ordinates for which hazard is available, to inelastic deformations is essential for most of the design procedures based on static or modal response analyses. This is carried out via strength, ductility, and oscillation period relationships (often referred to as *R-μ-T*) or simply based on the *equal displacement rule* (e.g., Veletsos and Newmark, 1960).

Available relations, for generality purposes, were calibrated in the past via regression of data from relatively limited ground motion sets (see also Vidic et al., 1994; Miranda and Bertero, 1994). These refer to single degree of freedom (SDoF) systems, typically with an elastic-plastic backbone[1], to which the structure of interest is somehow rendered equivalent during design.

The relationships between elastic and inelastic response, for practicality and manageability, are only taken in approximate format within codes, which often means to neglect significant associated uncertainty. In fact, recent attempts aim at performing probabilistic seismic hazard analysis (or PSHA, McGuire, 2004) directly in

[1] This is also because it has been found that the role of hysteresis shape may be minor.

terms of inelastic response. This would provide the seismic threat at a site by means of a parameter more informative for engineering practitioners.

Two possible approaches to incorporate nonlinear structural response in seismic hazard are: (1) to analytically model the inelastic to elastic response ratio (e.g., Tothong and Cornell, 2006); or (2) to develop prediction equations (or *attenuation models*) in terms on nonlinear response (e.g., Buratti et al., 2009; Bozorgnia et al., 2010a and 2010b). The latter approach is pursued in this study where relationships are developed for several nonlinear SDoFs, based on the large set of ground motion data contained in the ITalian ACcelerometric Archive or ITACA (Luzi at al. 2008; Pacor et al., 2011).

Estimating directly inelastic structural response rather than converting the elastic one, although equivalent in principle, may also allow to reduce the consequences of semi-empirical estimation issues propagating when predicting nonlinear behavior.

Considered SDoF systems include bilinear with hardening backbone with and without stiffness' degrading hysteretic behavior. Structural response measures (or engineering demand parameters, EDPs), despite previous work on the same topic, include both cyclic (e.g., energy dissipation) and peak response (e.g., maximum inelastic deformation) quantities. Elastic periods of SDOFs range in a broad interval sampled by 20 values. Level of nonlinearity is accounted for by considering one *strength reduction factors* ($R_s$) equal to 6.

The functional forms relating EDPs to source, site, and path characteristics are derived starting from those employed to compute the elastic IMs' attenuation relationships of Bindi et al. (2011). Preliminary, results refer to the geometric mean of the two horizontal components of ground motion.

In the following, details of the considered simple structural systems and response measures are given first. Then, the main features of the ground motion dataset are illustrated. Finally, the obtained equations for different nonlinear responses, and their dependency on the earthquake covariates, are discussed highlighting the use in the next generation of seismic hazard analysis, and as a benchmark for engineering validation of other types of ground motions obtained, for example, by means of physics-based simulations.

## 2 STRUCTURAL CASES AND RESPONSE MEASURES

The structural cases considered in this preliminary study were selected to emphasize both peak and cyclic response issues; thus two classes of hysteretic behaviors were selected. For each class of SDoFs, 20 elastic periods varying from 0.04s to 2s were considered, assuming the same sampling values selected in Bindi et al. (2011). The first structural behavior is represented by an elastic hardening backbone with the post-yielding stiffness assumed as 0.03 of the initial stiffness ($k_{el}$). These systems are characterized by a standard kinematic strain hardening hysteretic model (EPH-k), without any cyclic degradation, see Figure 1. This SDoF family is the same considered in the study by Tothong and Cornell (2006). The second structural behavior (EPH-p) features cyclic stiffness degradation, characterized by pinching hysteresis (Ibarra et al., 2005) and by the same elastic hardening backbone of the previous family of SDoFs; see Figure 2.

A single value of $R_s$ equal to 6 was considered being representative of a significant inelastic structural behavior. It is possible to achieve the same value of $R_s$ either for each record in a dataset (*constant R approach*) or on an average sense (*constant strength approach*) keeping constant the yielding strength. The former was adopted in this case, allowing every single record to show inelastic behavior in the SDoF. Therefore, the value of the yield strength ($F_y$) at a given oscillation period T is a record-specific quantity.

Two EDPs were selected to investigate both peak and cyclic seismic response. The displacement-based parameter is the peak inelastic displacement ($Sd_i$). The cyclic response-related parameter is the equivalent number of cycles ($N_e$). This latter is given by the cumulative hysteretic energy ($E_H$), evaluated as the sum of the areas of the hysteretic cycles (not considering contribution of viscous damping), normalized with respect to the largest cycle, evaluated as the area underneath the monotonic backbone curve from the yielding displacement to the peak inelastic displacement ($A_{plastic}$), see Equation (1). This allows separating peak demand, already

considered in the first EDP, from cyclic demand (Manfredi, 2001).

$$N_e = \frac{E_H}{A_{plastic}} \quad (1)$$

Once the peak and cyclic inelastic response to each single horizontal component of the record selected is evaluated according to the EDPs defined above, the geometric mean of the EDPs is considered for regression.

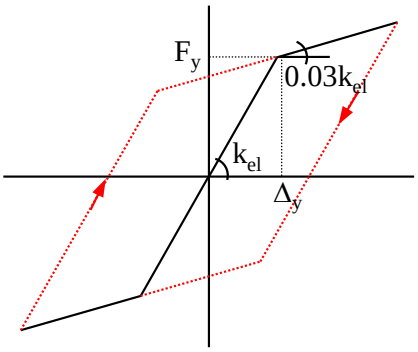


Figure 1. Elastic hardening monotonic backbone with standard kinematic strain hardening hysteretic model, (EPH-k).

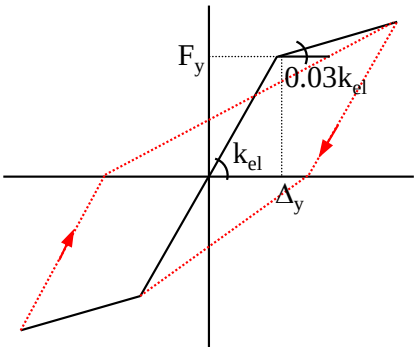


Figure 2. Elastic hardening monotonic backbone with pinching hysteresis featuring cyclic stiffness degradation, (EPH-p).

## 3 GROUND MOTION DATA

To compute peak and cyclic response parameters, the accelerograms corresponding to the strong ground-motion dataset used to develop the Italian Ground Motion Prediction Equations (ITA10, Bindi et al., 2011), were selected. The dataset is comprised of 769 records (three-components), with hypocentral depth within 30 km, and 150 stations over the magnitude range $4.1 \leq M_w \leq 6.9$ and distance, $R_{JB}$, range from 0 to 200 km (Figure 3). This dataset is extracted by the new Italian strong motion data base, ITACA (http//itaca.mi.ingv.it/) and includes all Italian events with $M_w > 4$ recorded from 1972 up to 2007 and the most relevant data from recent moderate earthquakes ($M_w$ = 6.3, 2009 L'Aquila and $M_w$ = 5.4, 2008 Parma) and aftershocks.

The development of ITA10 was feasible, thanks to the improvements in the quality and quantity of data and metadata in the new release of the ITACA database. In the selected dataset, distances larger than 10 km are well sampled over the entire magnitude range, while the recordings for distances shorter than 5 km are relevant in number for earthquakes with $M_w < 6$. All stations are classified following the Eurocode 8 or EC8 (CEN, 2004) scheme. The local site conditions values were obtained either from measurements or inferred by geological and geophysical data. Classes D and E (soft soils according to EC8) are poorly sampled, while the other classes are well represented with about 200 records in each class.

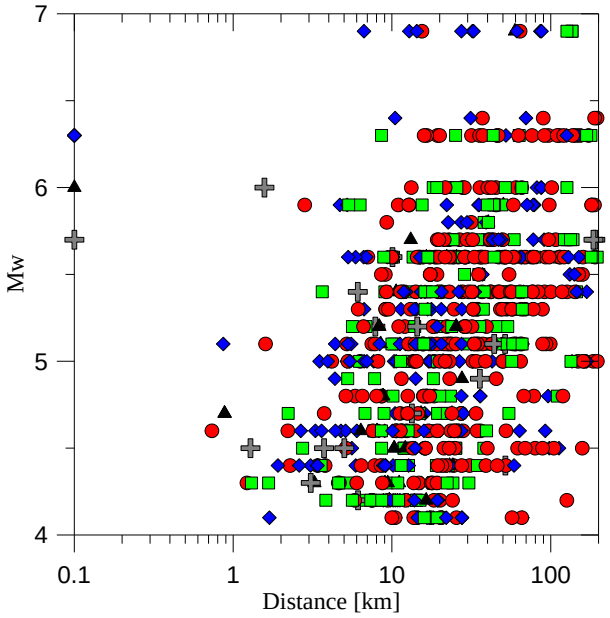


Figure 3. Magnitude versus distance plot. The data are grouped according to the EC8 site classification (A: red, B: blue; C: green, D: grey, E: black).

The accelerometric waveforms were downloaded from ITACA in the processed version form. The procedure for processing the data, consists in (Paolucci et al., 2011; Pacor et al., 2011): 1) baseline correction; 2) application of a cosine taper, based on the visual inspection of the record (typically between 2% and 5% of the total record length); records identified as late-triggered are not tapered; 3) visual inspection of the Fourier spectrum to select the band-pass frequency range; 4) application of a 2nd order a-causal time-domain Butterworth filter to the acceleration time-series padded with zeros; 5) double-integration to obtain displacement time series; 6) linear de-trending of displacement; 7) double-differentiation to get the corrected

acceleration. The applied procedure ensures the compatibility among acceleration, velocity and displacement time series.

A check on the displacement waveform resulting from the double-integration of the corrected accelerograms supported the choice of the high-pass corner frequency, $f_h$. Digital records are generally filtered with $f_h \leq 0.5$ Hz, down to values < 0.1 Hz (for the L'Aquila seismic sequence). On the other hand, analogue data, due to their lower quality, are generally high-pass filtered at frequencies higher than 0.2 Hz, with few exceptions, especially for large magnitude earthquakes.

## 4 RESULTS AND DISCUSSION

The equation used for the regression is similar to the model considered by Bindi et al. (2011) except for the exclusion of the style-of-faulting term and of a term linearly decreasing with distance (accounting for *anelastic attenuation*). Further tests will be performed to assess the effect of these simplifications.

Equation (2) shows the functional form considered in this study; $e_1$ is the constant term, $F_D(R,M)$, $F_M(M)$ and $F_s$ represent the distance (R) function, the magnitude (M) scaling and the site amplification correction, respectively. Magnitude measure is the moment magnitude ($M_w$), distance is the *Joyner-Boore distance* ($R_{JB}$), or the epicentral distance (in km), when the fault geometry is unknown (generally when $M_w$ <5.5). As mentioned, the structural response measures Y considered for the regressions are the peak inelastic displacement ($Sd_i$ in cm) and the equivalent number of cycles ($N_e$). The proposed equation for the distance function ($F_D$) is shown in equation (3), while the magnitude function ($F_M$) is shown in equation (4), where $M_{ref}$, $M_h$, $R_{ref}$ are coefficients to be determined through the analysis.

The term $F_S$ in equation (2) represents the site amplification and it is given by $F_S = s_j C_j$, for j=1,...5, where $s_j$ are the coefficients to be determined through the regression analysis, while $C_j$ are dummy variables used to denote the five different EC8 site classes (A to E).

The regressions are performed by applying a random effect approach (Abrahamson and Youngs, 1992) to the geometrical mean of the horizontal components. After some trial regressions and after Bindi et al. (2011) the following variables have been fixed: $R_{ref}$=1 km; $M_{ref}$=5;$M_h$=6.75; $b_3$=0. Overall, the model was calibrated over 11 period dependent parameters ($e_1$, $c_1$, $c_2$, h, $b_1$, $b_2$, $s_1$, $s_2$, $s_3$, $s_4$, $s_5$).

$$\log_{10} Y = e_1 + F_D(R,M) + F_M(M) + F_S \quad (2)$$

$$F_D(R,M) = \left[c_1 + c_2(M - M_{ref})\right]\log_{10}\left(\sqrt{R_{JB}^2 + h^2} / R_{ref}\right) \quad (3)$$

$$F_M(M) = \begin{cases} b_1(M - M_h) + b_2(M - M_h)^2 & \text{for M} \leq \text{M}_\text{h} \\ b_3(M - M_h) & \text{otherwise} \end{cases} \quad (4)$$

The regression coefficients for EPH-k and EPH-p systems, although should be taken as preliminary, are reported in Table 1 and Table 2 respectively, for both $Sd_i$ and $N_e$. For the sake of brevity the dependence on site condition is not discussed here (i.e., the results are presented for rock sites only, A site class). Thus, in equation (2), $F_s$=0 which means that we constrain the class A site to have no site amplification. In the following the mean estimates (and related standard deviations of the residuals) are discussed as a function of earthquake magnitude, source-to-site distance and oscillation period.

Figure 4 shows the residual distribution as function of the distance ($R_{JB}$) from the source and of the earthquake magnitude ($M_w$). Residuals are presented for $Sd_i$ and $N_e$ at two different periods and, as example, for the EPH-k systems. The distributions confirm that the derived models produce residuals independent on the explanatory variables.

The good performance of the predictive models is also confirmed by Figure 5 where the estimates for a magnitude 6.0 earthquake at two periods (T equal to 0.2 s and 1.0 s) are plotted as a function of distance.

The predictions are reported for both the considered systems (EPH-k and EPH-p) and they are compared with $Sd_i$ and $N_e$ data for a magnitude interval of 6.0±0.3.

The scaling with magnitude of the predictions for $Sd_i$ and $N_e$ is illustrated in Figure 6 for the EPH-k systems. The $Sd_i$ curves are also compared with the predictions for elastic spectral displacement (dashed lines) derived using the same functional form and the same magnitude-distance distribution of records, see Equation (2).

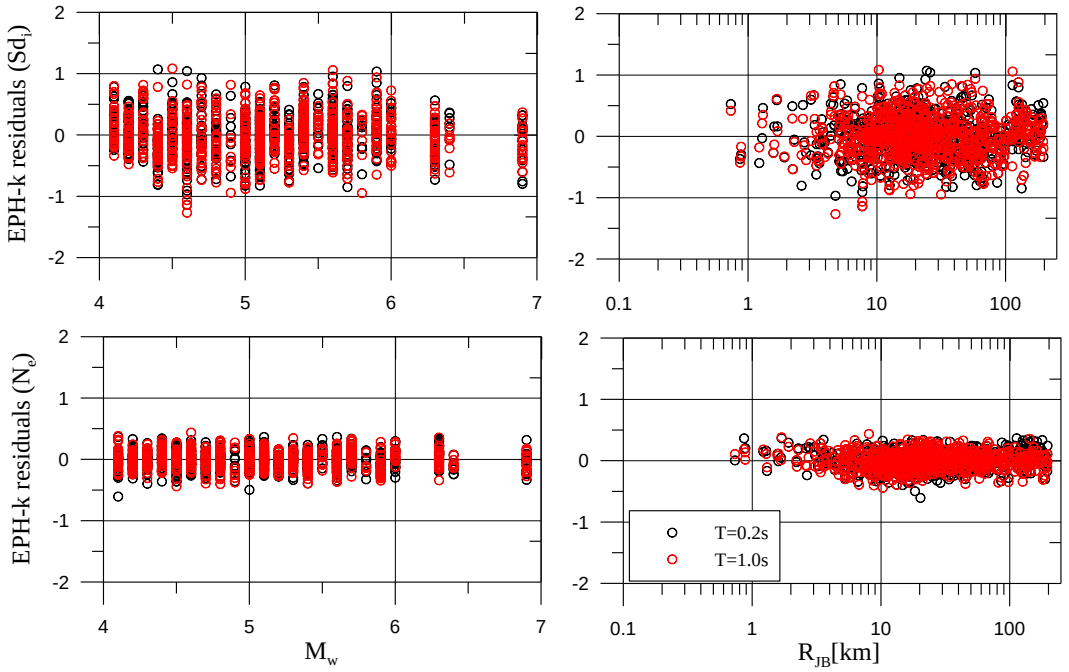


Figure 4. Residual distributions for EPH-k SDoFs as function of magnitude ($M_w$) and distance ($R_{JB}$) of the two EDPs considered in this study: $Sd_i$ for peak response and $N_e$ for cyclic response.

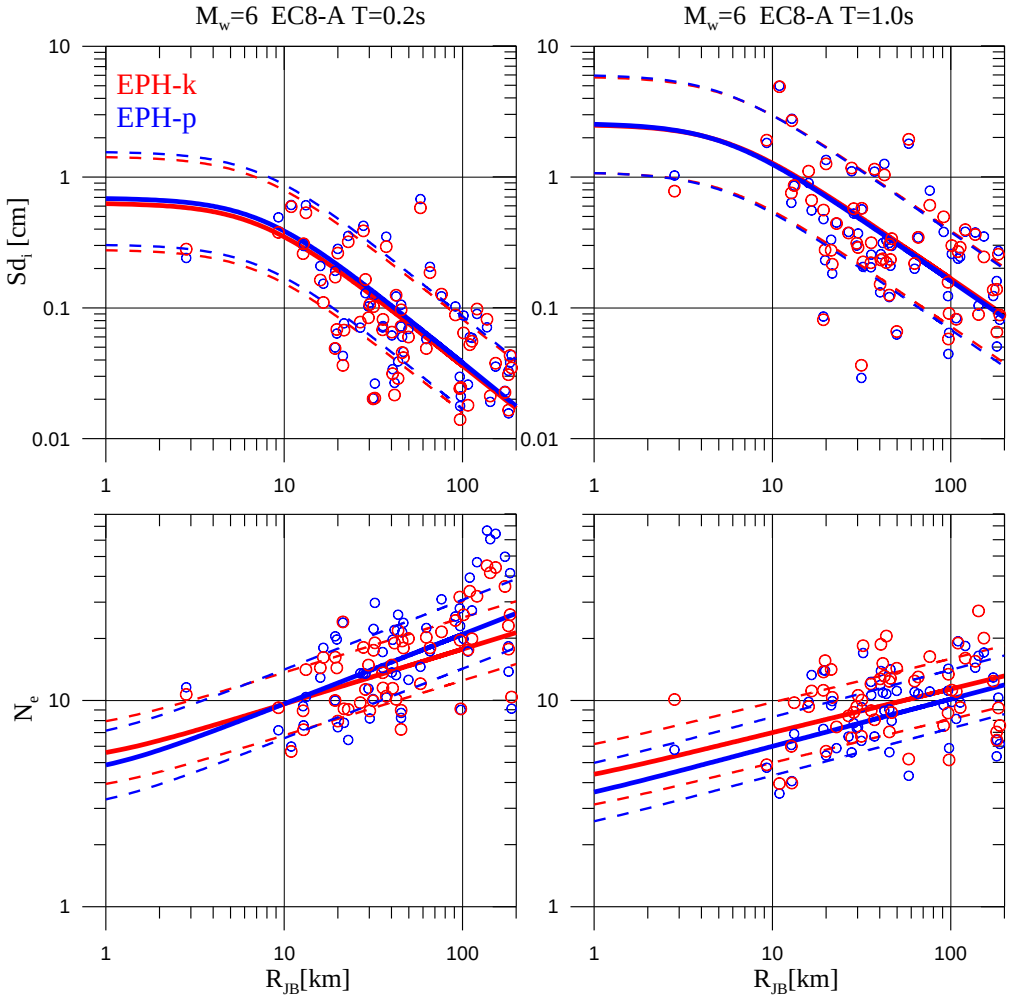


Figure 5. Estimates for a magnitude 6.0 earthquake at two natural periods (T=0.2s and 1.0s), plotted as a function of $R_{JB}$ and compared with $Sd_i$ and $N_e$ data for a magnitude interval of 6.0±0.3.

The difference between elastic and inelastic displacement is more evident at short periods (e.g., 0.2s) and moderate to large magnitudes ($M_w$ > 6), where larger values are predicted for the latter. At longer periods (e.g., 1.0s) elastic and inelastic spectral ordinates are comparable and for the largest magnitudes slightly larger elastic response is predicted.

$N_e$ regression is characterized by a dependence on magnitude less evident and differences in the mean prediction are relevant mostly for distances smaller than 10 km. The decreasing trend with increasing period of the cyclic response (recognizable from the comparison of the $N_e$ panels for different periods in Figure 6 and Figure 7) is typical of EDPs referring to cyclic response. Given the good correlation of $N_e$ with intensity measures related to ground motion duration, such as the so called Cosenza and Manfredi index ($I_D$), found in other studies (Iervolino et al., 2010a), the increasing trend of this EDP with distance can be easily justified, since this kind of IMs is characterized by the same increasing trend with distance, (see Iervolino et al. 2010b).

The magnitude dependency seems to be not very significant especially for medium to large distances; these results are in accordance with the findings of the $I_D$ attenuation relationship where magnitude coefficient is close to zero (Iervolino et al. 2010b). On the other hand $M_w$ effect on $N_e$ appears larger for small oscillation periods. For T = 1.0s there is an inversion of scaling for distances larger than 10 km. In fact, the $N_e$ trends with magnitude have to be assessed for statistical significance. Moreover, also suitability of the same functional form considered for peak displacement has to verified for EDPs related to cyclic structural response.

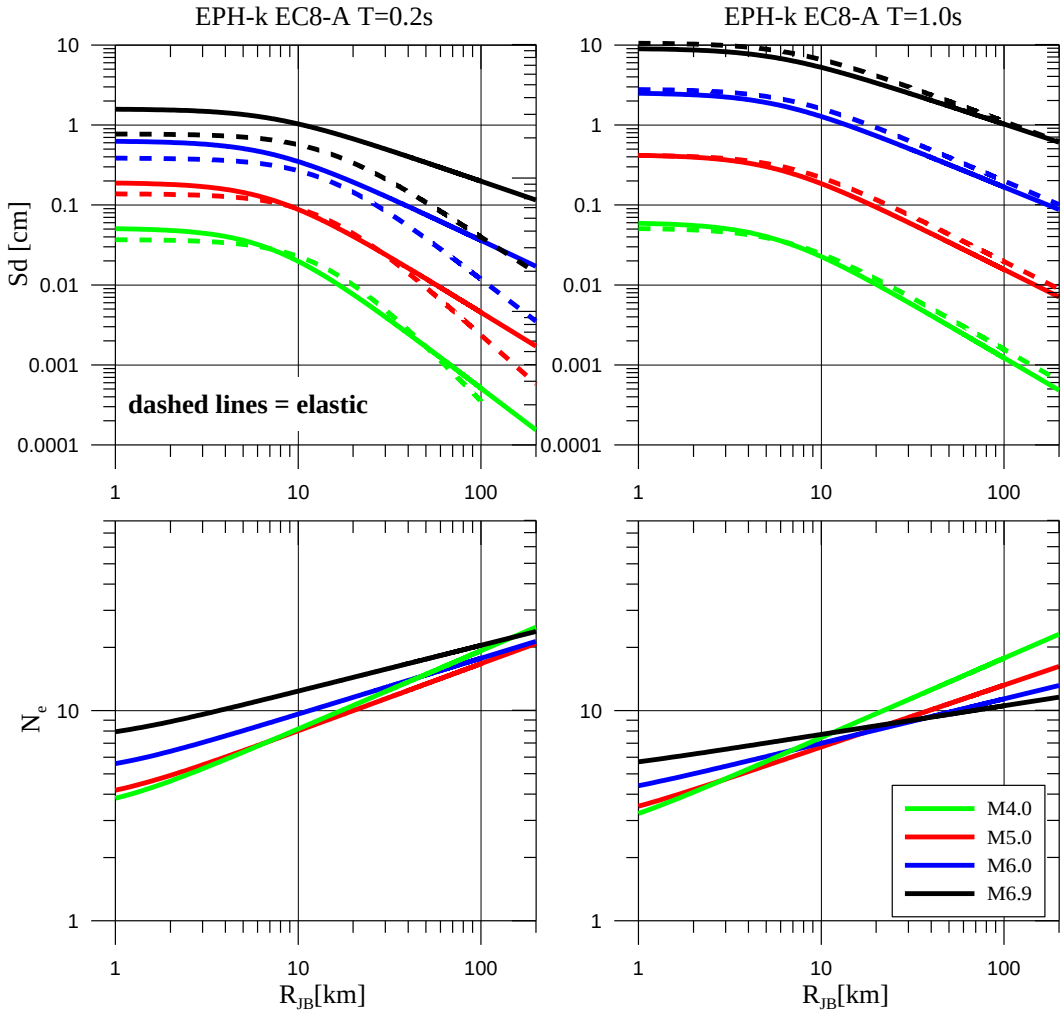


Figure 6. Scaling with magnitude of the predictions for $Sd_i$ and $N_e$ for EPH-k SdoF systems.

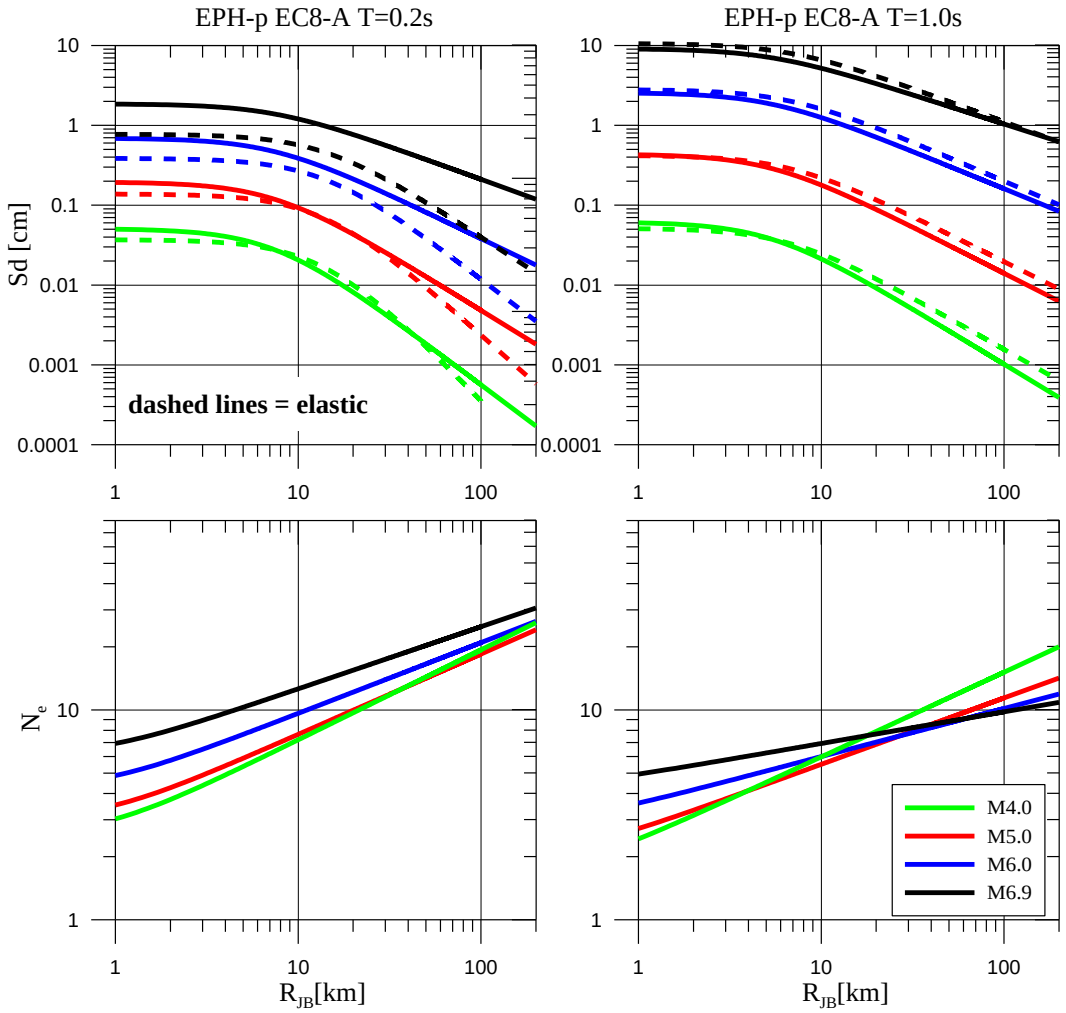


Figure 7. Scaling with magnitude of the predictions for $Sd_i$ and $N_e$ for EPH-p SdoF systems.

The standard deviation of residuals ($\sigma_{logY}$) associated to the mean predictions of the model presented in Equation (2), is shown in Figure 8, as a function of period, for all the considered structural response measures and for both EPH-k and EPH-p systems.

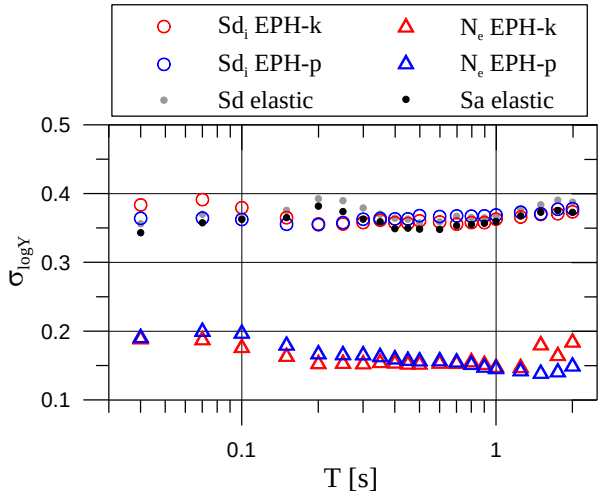


Figure 8. Standard deviation trends with periods of inelastic and elastic displacements, elastic acceleration (from Bindi et al., 2011) and equivalent number of cycles.

Moreover the $\sigma_{logY}$ for elastic spectral displacement (derived in this study) and for elastic spectral acceleration (from Bindi et al., 2011) are also shown as benchmark. The $Sd_i$ standard deviation varies from about 0.35 to 0.39 for EPH-k and from 0.35 to 0.37 for EPH-p. The values do not increase with respect to those derived for elastic acceleration and displacement spectra.

The $N_e$ standard deviation varies from about 0.14 to 0.19 for EPH-k and from 0.13 to 0.20 for EPH-p. Figure 9 shows the inelastic (and elastic) displacement and $N_e$ spectra predicted for a scenario earthquake ($M_w$ = 6.3 and $R_{JB}$ = 10 km) considering EPH-k and EPH-p systems. Inelastic spectrum predicts larger values than the elastic one for T < 0.5s, while for longer periods elastic spectrum is somewhat larger. No dependency on the hysteretic behavior of the two models is shown in peak response, as expected.

Considering cyclic response, $N_e$ spectra is slightly dependent from the hysteretic model; the curves for EPH-k and EPH-p are similar for T > 0.25s, whereas at shorter periods the EPH-p

model predicts larger values. The only stiffness degrading behavior (EPH-p) does not emphasize differences on cyclic response if compared to non-degrading hysteretic behavior (EPH-k), on the other hand when strength degradation is of concern the cyclic response dependence on hysteretic behavior can play a role in structural response (see Iervolino et al. 2010a). This latter issue highlights the necessity to consider further SDoF models characterized by strength degradation (softening in the monotonic backbone) to allow a more fulfilling characterization of predictive equations for cyclic response parameters.

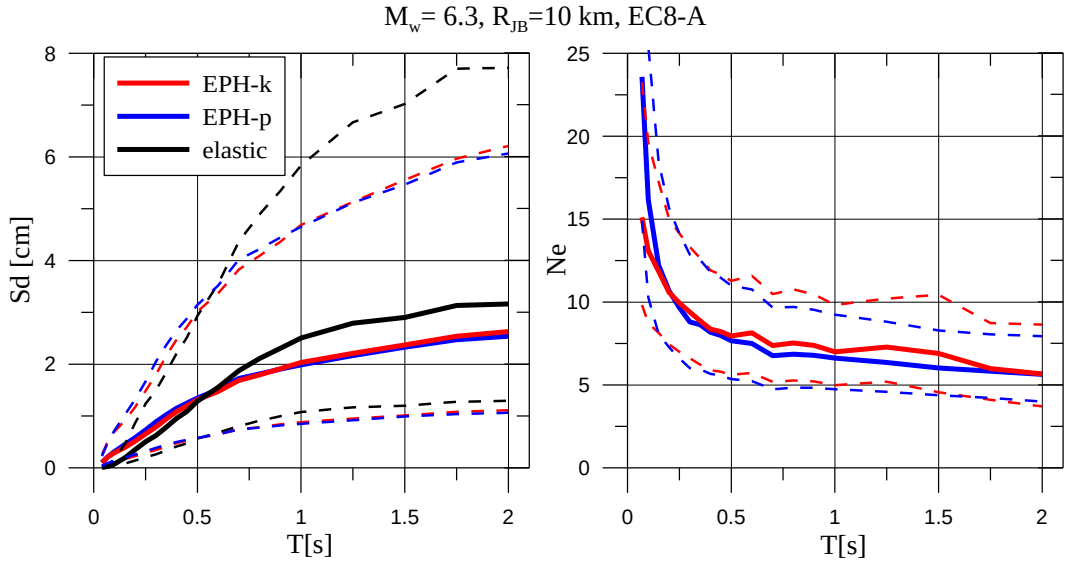


Figure 9. Mean inelastic and elastic displacement spectra (on the left) and Ne spectra (on the right) and their one standard deviation bands for EPH-k and EPH-p SDoFs, evaluated for a Mw = 6.3 and RJB = 10 km scenario.

Table 1. Regression coefficients and standard deviation for EPH-k SDoF, $R_s$ equal to 6 and A site class.

| T | $Sd_i$ | | | | | | | $N_e$ | | | | | | |
|---|---|---|---|---|---|---|---|---|---|---|---|---|---|---|
| | e1 | b1 | b2 | c1 | c2 | h | σ | e1 | b1 | b2 | c1 | c2 | h | σ |
| 0.04 | 0.6393 | -0.1313 | -0.0771 | -1.8482 | 0.3342 | 10.8708 | 0.3836 | 1.3678 | 0.4203 | 0.0568 | 0.3783 | -0.1242 | 0.2268 | 0.1883 |
| 0.07 | 0.8287 | 0.1037 | -0.0460 | -1.6128 | 0.2851 | 10.3363 | 0.3913 | 0.8954 | 0.2031 | 0.0313 | 0.4067 | -0.0292 | 0.2722 | 0.1871 |
| 0.10 | 0.7610 | 0.1511 | -0.0385 | -1.4768 | 0.2921 | 8.2848 | 0.3796 | 0.8893 | 0.2337 | 0.0337 | 0.3873 | -0.0473 | 0.4320 | 0.1758 |
| 0.15 | 0.7605 | 0.1641 | -0.0294 | -1.4082 | 0.3178 | 7.2440 | 0.3651 | 0.8963 | 0.2459 | 0.0446 | 0.3319 | -0.0408 | 0.6491 | 0.1630 |
| 0.20 | 0.8666 | 0.1793 | -0.0246 | -1.4091 | 0.3290 | 7.0687 | 0.3560 | 0.8742 | 0.2427 | 0.0440 | 0.3195 | -0.0533 | 0.8425 | 0.1524 |
| 0.25 | 0.9947 | 0.2496 | -0.0125 | -1.3905 | 0.3154 | 6.9055 | 0.3558 | 0.8515 | 0.2224 | 0.0348 | 0.3201 | -0.0625 | 0.7481 | 0.1528 |
| 0.30 | 1.0985 | 0.2749 | -0.0137 | -1.3889 | 0.3094 | 7.1412 | 0.3580 | 0.8324 | 0.2137 | 0.0315 | 0.3230 | -0.0716 | 0.6232 | 0.1521 |
| 0.35 | 1.2274 | 0.3362 | -0.0131 | -1.3722 | 0.2775 | 6.9974 | 0.3613 | 0.8062 | 0.1986 | 0.0273 | 0.3244 | -0.0758 | 0.4645 | 0.1539 |
| 0.40 | 1.3163 | 0.4024 | -0.0047 | -1.3469 | 0.2582 | 6.9916 | 0.3579 | 0.7573 | 0.1568 | 0.0187 | 0.3204 | -0.0681 | 0.6437 | 0.1533 |
| 0.45 | 1.3755 | 0.4445 | -0.0002 | -1.3265 | 0.2431 | 6.9669 | 0.3567 | 0.7333 | 0.1277 | 0.0084 | 0.3233 | -0.0666 | 0.9061 | 0.1517 |
| 0.50 | 1.4130 | 0.4634 | -0.0005 | -1.3126 | 0.2388 | 6.8387 | 0.3605 | 0.7071 | 0.1185 | 0.0073 | 0.3286 | -0.0644 | 1.0539 | 0.1516 |
| 0.60 | 1.4277 | 0.4529 | -0.0105 | -1.2876 | 0.2413 | 6.7518 | 0.3589 | 0.7642 | 0.1551 | 0.0126 | 0.3195 | -0.0815 | 0.6579 | 0.1529 |
| 0.70 | 1.4996 | 0.4990 | -0.0121 | -1.2566 | 0.2215 | 6.6382 | 0.3557 | 0.6712 | 0.1082 | 0.0079 | 0.3288 | -0.0663 | 1.3623 | 0.1527 |
| 0.80 | 1.4902 | 0.5055 | -0.0180 | -1.2175 | 0.2159 | 6.3076 | 0.3579 | 0.7192 | 0.1331 | 0.0117 | 0.3129 | -0.0756 | 0.9105 | 0.1551 |
| 0.90 | 1.5043 | 0.5087 | -0.0248 | -1.2012 | 0.2126 | 6.1107 | 0.3579 | 0.7048 | 0.1397 | 0.0178 | 0.3162 | -0.0722 | 0.8474 | 0.1512 |
| 1.00 | 1.5242 | 0.5380 | -0.0260 | -1.1717 | 0.2011 | 5.8697 | 0.3629 | 0.6487 | 0.1238 | 0.0167 | 0.3368 | -0.0711 | 2.9192 | 0.1473 |
| 1.25 | 1.5156 | 0.5321 | -0.0367 | -1.1392 | 0.2038 | 5.5071 | 0.3660 | 0.7503 | 0.1799 | 0.0314 | 0.2949 | -0.0834 | 0.4806 | 0.1466 |
| 1.50 | 1.5407 | 0.5729 | -0.0362 | -1.1029 | 0.1879 | 5.0325 | 0.3699 | 0.6970 | 0.1375 | 0.0200 | 0.2930 | -0.0721 | 0.9716 | 0.1797 |
| 1.75 | 1.5648 | 0.6035 | -0.0315 | -1.0873 | 0.1883 | 4.9134 | 0.3708 | 0.5241 | 0.0052 | 0.0065 | 0.2664 | -0.0105 | 1.5741 | 0.1641 |
| 2.00 | 1.5740 | 0.6157 | -0.0312 | -1.0784 | 0.1902 | 4.9658 | 0.3736 | 0.4535 | -0.0697 | 0.0007 | 0.2168 | 0.0386 | 1.2151 | 0.1837 |

Table 2. Regression coefficients and standard deviation for EPH-p SDoF, $R_s$ equal to 6 and A site class.

| T | $Sd_i$ | | | | | | | $N_e$ | | | | | | |
|---|---|---|---|---|---|---|---|---|---|---|---|---|---|---|
| | **e1** | **b1** | **b2** | **c1** | **c2** | **h** | **σ** | **e1** | **b1** | **b2** | **c1** | **c2** | **h** | **σ** |
| 0.04 | 0.5174 | -0.1475 | -0.0755 | -1.8239 | 0.3540 | 10.2344 | 0.3642 | 1.4544 | 0.4138 | 0.0514 | 0.4494 | -0.1363 | 0.1591 | 0.1904 |
| 0.07 | 0.8358 | 0.0800 | -0.0454 | -1.6542 | 0.3014 | 10.0682 | 0.3644 | 1.2132 | 0.4194 | 0.0560 | 0.4784 | -0.1091 | 0.6720 | 0.1994 |
| 0.10 | 0.8770 | 0.1613 | -0.0362 | -1.5273 | 0.2855 | 8.8291 | 0.3625 | 0.9722 | 0.3407 | 0.0503 | 0.4682 | -0.0682 | 0.1011 | 0.1967 |
| 0.15 | 0.9217 | 0.2179 | -0.0212 | -1.4422 | 0.2970 | 7.8474 | 0.3556 | 0.8195 | 0.2443 | 0.0400 | 0.4084 | -0.0306 | 0.8588 | 0.1793 |
| 0.20 | 0.9906 | 0.2404 | -0.0174 | -1.4156 | 0.3068 | 7.3514 | 0.3549 | 0.8036 | 0.2388 | 0.0371 | 0.3838 | -0.0458 | 0.8797 | 0.1666 |
| 0.25 | 1.0923 | 0.2987 | -0.0108 | -1.3847 | 0.2937 | 7.1025 | 0.3579 | 0.7625 | 0.2135 | 0.0313 | 0.3742 | -0.0480 | 0.9806 | 0.1653 |
| 0.30 | 1.1985 | 0.3512 | -0.0076 | -1.3670 | 0.2797 | 6.9907 | 0.3628 | 0.7215 | 0.1913 | 0.0245 | 0.3755 | -0.0553 | 0.6395 | 0.1651 |
| 0.35 | 1.2657 | 0.3659 | -0.0116 | -1.3570 | 0.2724 | 6.8822 | 0.3639 | 0.7583 | 0.2137 | 0.0253 | 0.3625 | -0.0723 | 0.6205 | 0.1625 |
| 0.40 | 1.3233 | 0.4104 | -0.0058 | -1.3394 | 0.2652 | 6.7909 | 0.3634 | 0.7186 | 0.1756 | 0.0153 | 0.3607 | -0.0699 | 0.6419 | 0.1592 |
| 0.45 | 1.3437 | 0.4216 | -0.0077 | -1.3196 | 0.2626 | 6.6437 | 0.3633 | 0.7165 | 0.1686 | 0.0110 | 0.3586 | -0.0766 | 0.6761 | 0.1572 |
| 0.50 | 1.3602 | 0.4338 | -0.0062 | -1.3066 | 0.2665 | 6.5278 | 0.3680 | 0.6909 | 0.1506 | 0.0062 | 0.3596 | -0.0766 | 0.8362 | 0.1563 |
| 0.60 | 1.3883 | 0.4419 | -0.0129 | -1.2801 | 0.2641 | 6.4350 | 0.3667 | 0.7103 | 0.1646 | 0.0096 | 0.3466 | -0.0843 | 0.6875 | 0.1565 |
| 0.70 | 1.4693 | 0.4934 | -0.0136 | -1.2521 | 0.2409 | 6.3539 | 0.3677 | 0.6244 | 0.1184 | 0.0047 | 0.3450 | -0.0673 | 1.1988 | 0.1549 |
| 0.80 | 1.4695 | 0.4896 | -0.0210 | -1.2334 | 0.2392 | 6.1461 | 0.3673 | 0.6618 | 0.1457 | 0.0110 | 0.3335 | -0.0742 | 0.8330 | 0.1512 |
| 0.90 | 1.4793 | 0.4963 | -0.0248 | -1.2184 | 0.2372 | 5.9864 | 0.3677 | 0.6751 | 0.1582 | 0.0144 | 0.3263 | -0.0782 | 0.6621 | 0.1473 |
| 1.00 | 1.4854 | 0.5085 | -0.0282 | -1.1967 | 0.2304 | 5.7153 | 0.3690 | 0.6638 | 0.1608 | 0.0189 | 0.3216 | -0.0742 | 0.6658 | 0.1450 |
| 1.25 | 1.4916 | 0.5089 | -0.0398 | -1.1656 | 0.2254 | 5.2469 | 0.3730 | 0.6895 | 0.2151 | 0.0363 | 0.3166 | -0.0873 | 0.4081 | 0.1419 |
| 1.50 | 1.5233 | 0.5562 | -0.0358 | -1.1356 | 0.2125 | 4.8475 | 0.3707 | 0.6660 | 0.2196 | 0.0416 | 0.3193 | -0.0884 | 0.4205 | 0.1384 |
| 1.75 | 1.5480 | 0.5828 | -0.0302 | -1.1275 | 0.2158 | 4.9016 | 0.3774 | 0.6766 | 0.2442 | 0.0498 | 0.3165 | -0.0983 | 0.3486 | 0.1404 |
| 2.00 | 1.5595 | 0.5956 | -0.0294 | -1.1188 | 0.2136 | 4.9221 | 0.3781 | 0.6723 | 0.2798 | 0.0630 | 0.3297 | -0.1061 | 0.1953 | 0.1489 |

## CONCLUSIONS

The possibility to develop prediction equations for nonlinear Single Degree of Freedom (SDoF) systems' responses based on the Italian Accelerometric Archive (ITACA) was explored in the study presented in this paper. Peak and cyclic inelastic structural response parameters were evaluated for the development of such attenuation models, useful for either design or assessment of structures. Two families of SDoF backbones were studied considering first a non-degrading behavior with a slight hardening in the backbone, and second a stiffness degrading behavior with the same hardening backbone of the first family.

A constant strength reduction factor approach was followed. In this preliminary enquiry only a single strength reduction factor equal to 6 was considered. Engineering demand parameters examined for regressions are the peak inelastic displacement and the equivalent number of cycles. The same functional form assumed in the traditional ground-motion attenuation models based on the same database was assumed.

The preliminary results indicate that the standard deviations of the regressions are very similar to the dispersion of GMPEs based on elastic parameters. This result may lead to a more accurate estimation of nonlinear response with respect to what done in current practice where estimates of inelastic structural demand (and associated uncertainty) are applied on top of elastic prediction equations.

Cyclic response evaluated in term of equivalent number of cycles showed similar trends with respect to those of duration-related measures. This result was expected according to the fair correlation found in other studies between those intensity measures and structural cyclic response. In fact, cyclic response prediction equation asks for further investigations since consolidated results are not available for this kind engineering demand parameters. On the other hand, this aspect can represent a useful tool especially when assessment of structural systems sensitive to cyclic response is of any concern.

Finally, it is to stress that results presented herein are preliminary and should be taken by the reader as qualitative and informative only. In fact, while it is expected that trends of EDPs versus IMs will be confirmed in the following of the study on this issue, it is likely that models' coefficient will change because of both more refinement of regression/dataset or changes of functional form of attenuation models.

## ACKNOWLEDGEMENTS

The analyses presented in this paper have been developed within the activities of the Rete dei Laboratori Universitari di Ingegneria Sismica – ReLUIS for the research program funded by the Dipartimento di Protezione Civile 2010-2013.

## REFERENCES

Abrahamson N.A., Youngs R.R., 1992. A stable algorithm for regression analyses using the random effects model. *Bulletin Seismological Society of America*, **82**, 505–510.

Bindi D., Pacor F., Luzi L., Puglia R., Massa M., Ameri G., Paolucci R., 2011. Ground motion prediction equations derived from the Italian strong motion database, *Bulletin of Earthquake Engineering* (under review).

Bozorgnia Y., Hachem M.M., Campbell K.W., 2010a. Ground motion prediction equation ("attenuation relationship") for inelastic response spectra. *Earthquake Spectra* **26**(1), 1-23.

Bozorgnia Y., Hachem M.M., Campbell K.W., 2010b. Deterministic and probabilistic predictions of yield strength and inelastic displacement spectra. *Earthquake Spectra* **26**(1), 25-40.

Buratti N., Savoia M., 2009. Using non-stationary artificial accelerograms for estimating maximum drift demands on R.C. frame structures. *XIII Convegno ANIDIS 2009- L'Ingegneria Sismica in Itali*a. Bologna. 28 June-2 July. ISBN: 978-88-904292-0-0.]

Comitè Europèen de Normalisation (CEN), 2004. *Eurocode 8 – Design of Structures for earthquake resistance – Part 1: General rules, seismic actions and rules for buildings*. EN 1998-1, CEN, Brussels.

Ibarra L.F., Medina R.A., Krawinkler H., 2005. Hysteretic models that incorporate strength and stiffness deterioration, *Earthquake Engineering and Structural Dynamics*, **34**, 1489-1511.

Iervolino I., De Luca F., Cosenza E., 2010a. Spectral shape-based assessment of SDOF nonlinear response to real, adjusted and artificial accelelrograms, *Engineering Structures*, 32, 2776-2792.

Iervolino I., Giorgio M., Galasso C., Manfredi G., 2010b. Conditional hazard maps for secondary intensity measures, *Bulletin of Seismological Society of America*, **100**(6), 3312-3319.

Luzi L., Hailemikael S., Bindi D., Pacor F., Mele F., Sabetta F., 2008. ITACA (ITalian ACelerometric Archieve): A web portal for the dissemination of Italian strong-motion data, *Seismological Research Letters*, **79**, 716-722.

Manfredi G., 2001. Evaluation of seismic energy demand, *Earthquake Engineering and Structural Dynamics*, **35**, 21–38.

McGuire R.K., 2004. *Seismic hazard and risk analysis*. Report MNO-10. Earthquake Engineering Research Institute Publication, Oakland, CA, USA.

Miranda E. and Bertero V.V., 1994. Evaluation of strength reduction factors for earthquake-resistant design. *Earthquake Spectra*, **10**(2), 357-379.

Pacor F, Paolucci R, Ameri G, Massa M, Puglia R, 2011. Italian strong motion records in ITACA: overview and record processing. *Bulletin of Earthquake Engineering* DOI: 10.1007/s10518-011-9295-x.

Paolucci R, Pacor F, Puglia R, Ameri G, Cauzzi C, Massa M., 2011. Record processing in ITACA, the new Italian strong-motion database. In: Akkar S, Gulkan P, Van Eck T (eds) Earthquake data in engineering seismology, geotechnical, geological and earthquake engineering series, vol 14, Chapter 8, pp 99–113. Springer, Berlin.

Tothong P., Cornell C.A:, 2006. An empirical ground-motion attenuation relation for inelastic spectral displacement. *Bulletin of the Seismological Society of America*, **96**(6), 2146-2164.

Veletsos A.S., Newmark N.M., 1960. Effect of inelastic behavior on the response of simple systems to earthquake motions, *Proccedings of the 2nd World Conference on Earthquake Engineeirng*, Tokyo, Japan, 895-912.

Vidic T., Fajfar P., Fischinger M., 1994. Consistent inelastic design spectra: strength and displacement. *Earthquake Engineering and Structural Dynamics*, **23**, 507-521.